This paper is published as part of a *Nanoscale* themed issue on doped nanostructures

Guest Editor: Stephen Pearton

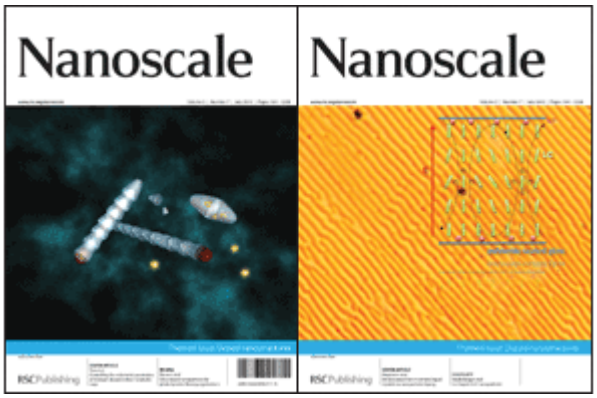

Editorial

Doped nanostructures
Stephen Pearton, *Nanoscale*, 2010
DOI: 10.1039/c005273f

Review Articles

Impacts of doping on thermal and thermoelectric properties of nanomaterials
Gang Zhang and Baowen Li, *Nanoscale*, 2010
DOI: 10.1039/c0nr00095g

Effect of N/B doping on the electronic and field emission properties for carbon nanotubes, carbon nanocones, and graphene nanoribbons
Shan-Sheng Yu and Wei-Tao Zheng, *Nanoscale*, 2010
DOI: 10.1039/c0nr00002g

Silica-based nanoparticles for photodynamic therapy applications
Pierre Couleaud, Vincent Morosini, Céline Frochot, Sébastien Richeter, Laurence Raehm and Jean-Olivier Durand, *Nanoscale*, 2010
DOI: 10.1039/c0nr00096e

Mini Review

Co-Doped ZnO nanoparticles: Minireview
Igor Djerdj, Zvonko Jagli?i?, Denis Ar?on and Markus Niederberger, *Nanoscale*, 2010
DOI: 10.1039/c0nr00148a

Communications

Controlling the volumetric parameters of nitrogen-doped carbon nanotube cups
Brett L. Allen, Matthew B. Keddie and Alexander Star, *Nanoscale*, 2010
DOI: 10.1039/c0nr00043d

Visible light induced photobleaching of methylene blue over melamine-doped TiO_2 nanocatalyst
Jurate Virkutyte, Babita Baruwati and Rajender S. Varma, *Nanoscale*, 2010
DOI: 10.1039/c0nr00089b

Selective detection of trace amount of Cu^{2+} using semiconductor nanoparticles in photoelectrochemical analysis
Guang-Li Wang, Jing-Juan Xu and Hong-Yuan Chen, *Nanoscale*, 2010
DOI: 10.1039/c0nr00084a

Flower-like TiO_2 nanosructures with exposed {001} facets: Facile synthesis and enhanced photocatalysis
Min Liu, Lingyu Piao, Weiming Lu, Siting Ju, Lei Zhao, Chunlan Zhou, Hailing Li and Wenjing Wang, *Nanoscale*, 2010
DOI: 10.1039/c0nr00050g

Papers

Electroconvection in nematic liquid crystals *via* nanoparticle doping
Martin Urbanski, Brandy Kinkead, Hao Qi, Torsten Hegmann and Heinz-S. Kitzerow, *Nanoscale*, 2010
DOI: 10.1039/c0nr00139b

Superhydrophilicity-assisted preparation of transparent and visible light activated N-doped titania film
Qing Chi Xu, Diana V. Wellia, Rose Amal, Dai Wei Liao, Say Chye Joachim Loo and Timothy Thatt Yang Tan, *Nanoscale*, 2010
DOI: 10.1039/c0nr00105h

The influence of doping on the device characteristics of $In_{0.5}Ga_{0.5}As/GaAs/Al_{0.2}Ga_{0.8}As$ quantum dots-in-a-well infrared photodetectors
G. Jolley, L. Fu, H. H. Tan and C. Jagadish, *Nanoscale*, 2010
DOI: 10.1039/c0nr00128g

Study of concentration-dependent cobalt ion doping of TiO_2 and $TiO_{2-x}N_x$ at the nanoscale
James L. Gole, Sharka M. Prokes, O. J. Glembocki, Junwei Wang, Xiaofeng Qiu and Clemens Burda, *Nanoscale*, 2010
DOI: 10.1039/c0nr00125b

Multifunctional nanocomposites of superparamagnetic (Fe_3O_4) and NIR-responsive rare earth-doped up-conversion fluorescent ($NaYF_4$: Yb,Er) nanoparticles and their applications in biolabeling and fluorescent imaging of cancer cells
Congcong Mi, Jingpu Zhang, Huanyu Gao, Xianlong Wu, Meng Wang, Yingfan Wu, Yueqin Di, Zhangrun Xu, Chuanbin Mao and Shukun Xu, *Nanoscale*, 2010
DOI: 10.1039/c0nr00102c

Effect of doping on the morphology and multiferroic properties of $BiFeO_3$ nanorods
Dimple P. Dutta, O. D. Jayakumar, A. K. Tyagi, K. G. Girija, C. G. S. Pillai and G. Sharma, *Nanoscale*, 2010
DOI: 10.1039/c0nr00100g

Effect of substrate temperature on implantation doping of Co in CdS nanocrystalline thin films
S. Chandramohan, A. Kanjilal, S. N. Sarangi, S. Majumder, R. Sathyamoorthy, C.-H. Hong and T. Som, *Nanoscale*, 2010
DOI: 10.1039/c0nr00123f

Modification of neodymium-doped ZnO hybrid nanoparticles under mild hydrothermal conditions
Behzad Shahmoradi, K. Soga, S. Ananda, R. Somashekar and K. Byrappa, *Nanoscale*, 2010
DOI: 10.1039/c0nr00069h

***Ex situ* vapor phase boron doping of silicon nanowires using BBr_3**
Gregory S. Doerk, Gabriella Lestari, Fang Liu, Carlo Carraro and Roya Maboudian, *Nanoscale*, 2010
DOI: 10.1039/c0nr00127a

Change in conformation of polymer PFO on addition of multiwall carbon nanotubes
Malti Bansal, Ritu Srivastava, C. Lal, M. N. Kamalasanan and L. S. Tanwar, *Nanoscale*, 2010
DOI: 10.1039/c0nr00001a

Amino acid-assisted one-pot assembly of Au, Pt nanoparticles onto one-dimensional ZnO microrods
Xianghong Liu, Jun Zhang, Xianzhi Guo, Shihua Wu and Shurong Wang, *Nanoscale*, 2010
DOI: 10.1039/c0nr00015a

Luminescence resonance energy transfer from an upconverting nanoparticle to a fluorescent phycobiliprotein
Fiorenzo Vetrone, Rafik Naccache, Christopher G. Morgan and John A. Capobianco, *Nanoscale*, 2010
DOI: 10.1039/c0nr00126k

Doping single-walled carbon nanotubes through molecular charge-transfer: a theoretical study
Arun K. Manna and Swapan K. Pati, *Nanoscale*, 2010
DOI: 10.1039/c0nr00124d

Energy transfer study between Ce^{3+} and Tb^{3+} ions in doped and core-shell sodium yttrium fluoride nanocrystals
Pushpal Ghosh, Arik Kar and Amitava Patra, *Nanoscale*, 2010
DOI: 10.1039/c0nr00019a

Pt surface modification of SnO_2 nanorod arrays for CO and H_2 sensors
Hui Huang, C. Y. Ong, J. Guo, T. White, M. S. Tse and O. K. Tan, *Nanoscale*, 2010
DOI: 10.1039/c0nr00159g

Poly (acrylic acid)-capped lanthanide-doped BaFCl nanocrystals: synthesis and optical properties
Qiang Ju, Wenqin Luo, Yongsheng Liu, Haomiao Zhu, Renfu Li and Xueyuan Chen, *Nanoscale*, 2010
DOI: 10.1039/c0nr00116c

Enhanced Cu emission in ZnS : Cu,Cl/ZnS core–shell nanocrystals
Carley Corrado, Morgan Hawker, Grant Livingston, Scott Medling, Frank Bridges and Jin Z. Zhang, *Nanoscale*, 2010
DOI: 10.1039/c0nr00056f

Synthesis and characterization of zirconium-doped mesoporous nano-crystalline TiO_2
Kanattukara Vijayan Bineesh, Dong-Kyu Kim and Dae-Won Park, *Nanoscale*, 2010
DOI: 10.1039/c0nr00108b

Zn-doped nanocrystalline TiO_2 films for CdS quantum dot sensitized solar cells
Guang Zhu, Zujun Cheng, Tian Lv, Likun Pan, Qingfei Zhao and Zhuo Sun, *Nanoscale*, 2010
DOI: 10.1039/c0nr00087f

Effect of synergy on the visible light activity of B, N and Fe co-doped TiO_2 for the degradation of MO
Mingyang Xing, Yongmei Wu, Jinlong Zhang and Feng Chen, *Nanoscale*, 2010
DOI: 10.1039/c0nr00078g

Facile synthesis of lanthanide nanoparticles with paramagnetic, down- and up-conversion properties
Zhengquan Li and Yong Zhang, *Nanoscale*, 2010
DOI: 10.1039/c0nr00073f

Glucose oxidase-doped magnetic silica nanostrutures as labels for localized signal amplification of electrochemical immunosensors
Jingjing Ren, Dianping Tang, Biling Su, Juan Tang and Guonan Chen, *Nanoscale*, 2010
DOI: 10.1039/b9nr00416e

The role of ellipticity on the preferential binding site of Ce and La in C_{78}-D_{3h}—A density functional theory study
K. Muthukumar and J. A. Larsson, *Nanoscale*, 2010
DOI: 10.1039/c0nr00021c

Tuning the shape and thermoelectric property of PbTe nanocrystals by bismuth doping
Qian Zhang, Ting Sun, Feng Cao, Ming Li, Minghui Hong, Jikang Yuan, Qingyu Yan, Huey Hoon Hng, Nianqiang Wu and Xiaogang Liu, *Nanoscale*, 2010
DOI: 10.1039/c0nr00115e

Flower-like TiO_2 nanostructures with exposed {001} facets: Facile synthesis and enhanced photocatalysis†

Min Liu,[a] Lingyu Piao,*[b] Weiming Lu,[ac] Siting Ju,[b] Lei Zhao,[a] Chunlan Zhou,[a] Hailing Li[a] and Wenjing Wang*[a]

Received (in Gainesville, FL, USA) 24th January 2010, Accepted 17th February 2010
First published as an Advance Article on the web 17th March 2010
DOI: 10.1039/c0nr00050g

Flower-like TiO_2 nanostructures with exposed {001} facets were synthesized by a low-temperature hydrothermal process from Ti powders for the first time, and they exhibited enhanced photocatalytic degradation of methylene blue dye under ultraviolet light irradiation.

Titanium oxide (TiO_2), as one of the most important oxides, has been widely investigated due to its numerous applications in photovoltaic cells,[1] photocatalysis,[2,3] Li-ion battery materials,[4] sensors[5] and so on. These applications originate from the unique physical and chemical properties of TiO_2 which depend not only on the crystal phase and particle size but also on the exposed facet.[6–10] For anatase TiO_2, both theoretical and experimental studies have found that the minority {001} facets in the equilibrium state are especially reactive.[8–11] However, it has been demonstrated that the average surface energies are $\gamma_{\{001\}}$ (0.90 J m^{-2}) > $\gamma_{\{100\}}$ (0.53 J m^{-2}) > $\gamma_{\{101\}}$ (0.44 J m^{-2}).[7,9,10] Although the higher-surface-energy {001} facets have much higher chemical activities, almost all of anatase TiO_2 micro- and nanostructures reported to date are usually dominated by less-reactive {101} facets, which are thermodynamically stable due to their lower surface energy. Therefore, anatase TiO_2 nanostructures with exposed {001} facets are rarely observed.

An important step forward in the preparation of anatase TiO_2 single crystals with exposed {001} facets were achieved by Lu and co-workers.[11] They reported the synthesis of anatase TiO_2 microcrystals with exposed {001} facets by using TiF_4 as the raw material. Since then, several researchers have prepared anatase TiO_2 single crystals with exposed {001} facets from different raw materials, such as titanium tetrafluorine, titanium chloride, tetrabutyl titanate, titanium tetraisopropoxide, and so on.[12–16] However, these materials have high hydrolytic reaction rates which make it difficult to control their reaction processes. Very recently, anatase TiO_2 sheets with a high percentage of {001} facets were prepared from titanium nitride by Lu and co-workers.[17] However, the price of titanium nitride is still very high. Moreover, all of the previously mentioned experimental processes require high temperatures,[11–18] even as high as 1300 °C,[15] which not only increases the production cost but also hinders scaled-up production.

Furthermore, nanomaterials with hierarchical architectures have attracted much attention, since they can possess a number of attractive properties and have a wide range of applications in catalysis, solar cells, Li-ion batteries, and so on.[19–24] For example, rose-like ZnO nanostructures, which consist of many nanosheets, exhibit enhanced light conversion efficiency in dye-sensitized solar cells (DSSC).[23] Flower-like $ZnMn_2O_4$ nanostructures, which are composed of numerous nanorods, showed enhanced electrochemical lithium storage.[24] However, it remains a great challenge to develop feasible methods for the synthesis of well-defined hierarchical TiO_2 nanostructures.

Herein, we report a simple and facile route for the one-pot synthesis of flower-like TiO_2 nanostructures with exposed {001} facets by a low-temperature hydrothermal process from Ti powders. These flower-like TiO_2 nanostructures with exposed {001} facets have never been reported until now. In agreement with calculations, it can be confirmed that these flower-like TiO_2 nanostructures contain about 10–30% exposed highly reactive {001} facets. Moreover, these flower-like TiO_2 nanostructures exhibited enhanced photocatalytic degradation of methylene blue (MB) dye under ultraviolet (UV) light irradiation, and they also have potential applications in photonic and optoelectronic devices, solar cells, sensors, and so on.

In a typical synthesis, 0.1 g Ti powder (200 mesh, 99.9% purity, see Fig. S1 of the ESI†), 40 ml H_2O and 0.25 ml hydrofluoric acid (40 wt %) were added into a Teflon-lined autoclave. Then, the mixture was kept at 120 °C for 10 h. After completion of the reaction, the products were collected by centrifugation and thoroughly washed with high-purity water (18 MΩ) until pH 7.0 was reached. Finally, the products were dried at 80 °C.

Fig. 1 a and b show typical field-emission scanning electron microscope (FE-SEM) images of the flower-like TiO_2 nanostructures. It can be seen that the TiO_2 product contains numerous flower-like aggregates, and almost all of them show the same morphology. These flower-like TiO_2 nanostructures have a size around 300–700 nm, and they are composed of large numbers of truncated tetragonal pyramidal TiO_2 nanocrystals. The width of their top surface is *ca.* 50–150 nm. The length of the truncated tetragonal pyramidal TiO_2 nanocrystals is *ca.* 100–200 nm. Fig. 1c shows an X-ray diffraction (XRD) pattern of the flower-like TiO_2 nanostructures. All XRD peaks of the synthesized flower-like TiO_2 nanostructures can be indexed to the anatase TiO_2 phase (JCPDS No. 21-1272) and no residual Ti phase can be detected. Remarkably enhanced (101) and

[a]*Key Laboratory of Solar Thermal Energy and Photovoltaic System, Institute of Electrical Engineering, Chinese Academy of Sciences, No. 6 Beiertiao, Zhongguancun, 100190 Beijing, China. E-mail: wjwangwj@126.com; Fax: (+86) 10-82547041; Tel: (+86) 10-82547042*
[b]*National Center for Nanoscience and Technology, No.11 Beiyitiao, Zhongguancun, 100190 Beijing, China. E-mail: piaoly@nanoctr.cn; Fax: (+86) 10-82545505; Tel: (+86) 10-82545505*
[c]*Institute of Metal Research, Chinese Academy of Sciences, Shenyang, 110016, China*
† Electronic supplementary information (ESI) available: Additional FE-SEM images. See DOI: 10.1039/c0nr00050g

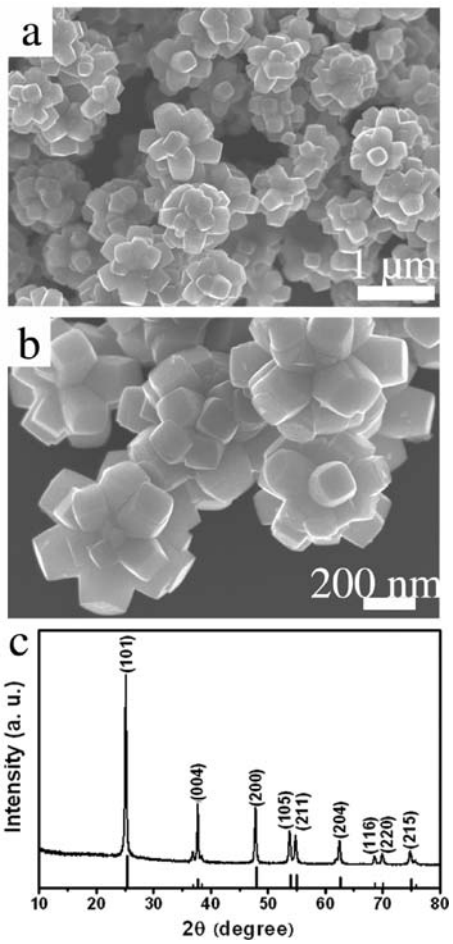

Fig. 1 (a, b) FE-SEM images of the flower-like TiO_2 nanostructures at low and high magnifications, respectively. (c) XRD pattern of the flower-like TiO_2 nanostructures. Vertical bars indicate peak position and intensity of anatase TiO_2 (JCPDS No. 21-1272).

(004) peaks indicate that the TiO_2 nanostructures are dominant in {101} and {001} facets.

Fig. 2a shows a transmission electron microscopy (TEM, FEI F-20) image of the flower-like TiO_2 nanostructures. It confirms that the flower-like TiO_2 nanostructures were composed of many truncated tetragonal pyramidal TiO_2 nanocrystals. An angle of 68.3° ± 0.3°, which is consistent with the interfacial angle between (001) and (101),[11,14,15] was observed on the truncated tetragonal pyramidal TiO_2 nanocrystals. It suggests that the truncated tetragonal pyramidal TiO_2 nanocrystals expose facets of {001} and {101}. Fig. 2b gives a schematic illustration of the flower-like TiO_2 nanostructures. Fig. 2c shows a high-resolution TEM (HRTEM) image of a truncated tetragonal pyramidal TiO_2 nanocrystal with clear crystalline lattice fringes. The lattice spacing of 0.352 nm corresponds to the {101} planes, while the lattice spacing of 0.237 nm corresponds to the {004} planes. The angle labeled in the corresponding fast-Fourier transform (FFT) image (Fig. 2d) is 68.3° ± 0.3°, which is identical to the theoretical value for the angle between the {101} and {001} facets. On the basis of the above characterizations, it can be confirm that the flower-like TiO_2 nanostructures have exposed {001} facets.

It has been demonstrated that metal Ti could react with HF forming TiO_2, under hydrothermal conditions.[25] Due to their low

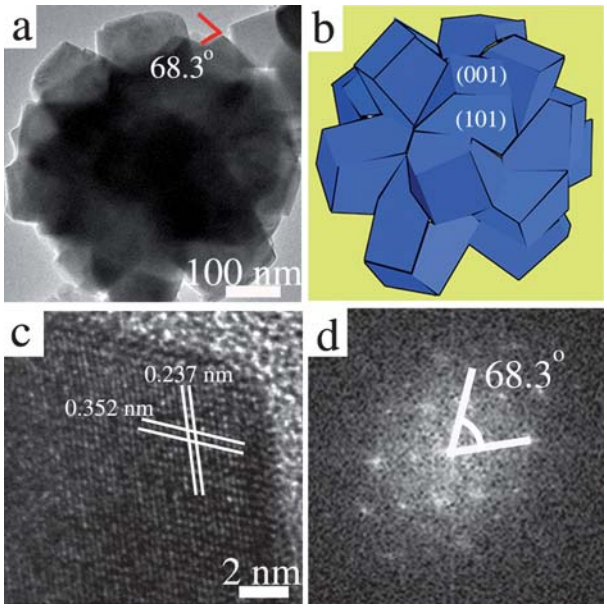

Fig. 2 (a) TEM image of the flower-like TiO_2 nanostructures. (b) Schematic diagram of the flower-like TiO_2 nanostructures. (c) HRTEM image of a truncated tetragonal pyramidal TiO_2 nanocrystal. (d) The corresponding fast-Fourier transform (FFT) pattern.

surface energy, TiO_2 crystals grow with exposed {101} facets mainly during the early stages of synthesis. However, fluorine ions can markedly reduce the surface energy of {001} facets to a level lower than that of {101} facets.[11] As a result, {001} facets are exposed during growth, and flower-like TiO_2 nanostructures with exposed {001} facets are formed. Therefore, hydrofluoric acid is believed to have a triple role here: to dissolve the Ti powders, to retard the hydrolysis of the titanium precursor, and to reduce the surface energy.[18]

The photocatalytic activity of the flower-like TiO_2 nanostructures was evaluated in terms of the decolorization of MB dye under UV light irradiation. For photocatalytic reaction, the surface fluorine was removed using a heat treatment process at 600 °C in O_2 for 2 h, without altering the morphology (see Fig. S2 of the ESI†). After that, 30 mg flower-like TiO_2 nanostructures was dispersed in 100 ml of aqueous solution containing 0.01 M NaOH and 25 ppm MB.[12] Before exposure to UV light irradiation, the suspension was stirred in the dark for 1 h to allow it reach a complete adsorption–desorption equilibrium. Then the solution was irradiated with ~0.5 mW cm^{-2} UV light (with a wavelength peak at 365 nm) under continuous stirring. The concentration of MB was determined from the absorbance at the wavelength of 665 nm. For comparison, the same procedure was also done for P25 TiO_2 powders.

As shown in Fig. 3, the flower-like TiO_2 nanostructures exhibited higher activity than that of the commercial P25 TiO_2 powders. The linear relationship of ln C_0/C *vs.* time (inset of Fig. 3) shows that the photocatalytic degradation of MB follows pseudo-first-order kinetics, $\ln(C_0/C) = kt$, where C/C_0 is the normalized MB concentration, t is the reaction time, and k is the pseudo-first-rate constant. The apparent photochemical degradation rate constant for the flower-like TiO_2 nanostructures is 1.23×10^{-2} min^{-1}, which is almost two times of that for the P25 TiO_2 powders, 6.73×10^{-3} min^{-1}. This further confirms that the flower-like TiO_2 nanostructures exhibit high photocatalytic efficiency. The enhanced photocatalytic activity of the flower-like TiO_2 nanostructures can be attributed to their

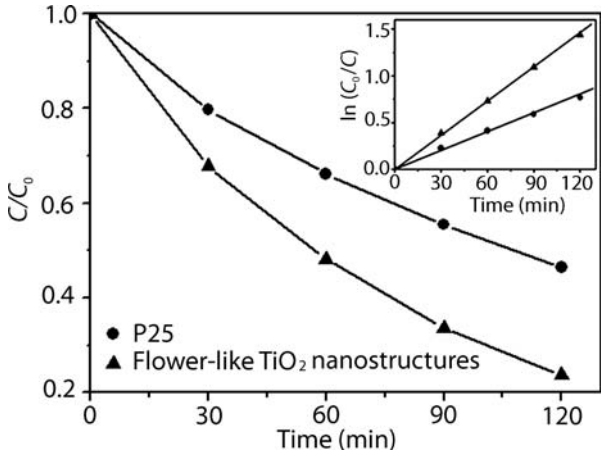

Fig. 3 The variation of MB concentration by photoelectrocatalytic reaction with P25 TiO_2 powders and flower-like TiO_2 nanostructures. The inset shows the pseudo-first-order kinetic rate plots for the photochemical degradation of MB.

three-dimensional (3D) hierarchical nanostructures and exposed {001} facets. 3D hierarchical nanostructures are regarded to have a greater number of active sites than either 1D or 0D architectures.[26,27] Furthermore, it has been demonstrated that the {001} facets are more reactive toward dissociative adsorption of reactant molecules compared with {101} facets.[28–32] Therefore, high photocatalytic efficiency is expected for the flower-like TiO_2 nanostructures with {001} facets.

In conclusion, flower-like TiO_2 nanostructures with exposed {001} facets have been successfully synthesized by a low-temperature hydrothermal process from Ti powders for the first time. Owing to their chemically active {001} facets, these TiO_2 nanostructures exhibited enhanced photocatalytic efficiency, and they could possibly be further used in photovoltaic cells, photonic and optoelectronic devices, sensors and so on.

Acknowledgements

This work was supported by the National Natural Science Foundation of China under Grant Nos 60576065 and 50602008, the Knowledge Innovation Program of the Chinese Academy of Sciences under Grant No. KGCXZ-YW-351, and the National High-Technology Research and Development Programme of China under Grant Nos 2006AA05Z405 and 2007AA05Z437.

References

1 B. O'Regan and M. Gratzel, *Nature*, 1991, **353**, 737.
2 A. Fujishima and K. Honda, *Nature*, 1972, **238**, 37.
3 A. L. Linsebigler, G. Q. Lu and J. T. Yates, *Chem. Rev.*, 1995, **95**, 735.
4 V. Subramanian, A. Karki, K. I. Gnanasekar, F. P. Eddy and B. Rambabu, *J. Power Sources*, 2006, **159**, 186.
5 N. Wu, S. Wang and I. A. Rusakova, *Science*, 1999, **285**, 1375.
6 X. B. Chen and S. S. Mao, *Chem. Rev.*, 2007, **107**, 2891.
7 U. Diebold, *Surf. Sci. Rep.*, 2003, **48**, 53.
8 X. Gong and A. Selloni, *J. Phys. Chem. B*, 2005, **109**, 19560.
9 M. Lazzeri, A. Vittadini and A. Selloni, *Phys. Rev. B: Condens. Matter Mater. Phys.*, 2001, **63**, 155409.
10 M. Lazzeri, A. Vittadini and A. Selloni, *Phys. Rev. B: Condens. Matter Mater. Phys.*, 2002, **65**, 119901.
11 H. G. Yang, C. H. Sun, S. Z. Qiao, J. Zou, G. Liu, S. C. Smith, H. M. Cheng and G. Q. Lu, *Nature*, 2008, **453**, 638.
12 H. G. Yang, G. Liu, S. Z. Qiao, C. H. Sun, Y. G. Jin, S. C. Smith, J. Zou, H. M. Cheng and G. Q. Lu, *J. Am. Chem. Soc.*, 2009, **131**, 4078.
13 X. Han, Q. Kuang, M. Jin, Z. Xie and L. Zheng, *J. Am. Chem. Soc.*, 2009, **131**, 3152.
14 Y. Dai, C. M. Cobley, J. Zeng, Y. M. Sun and Y. Xia, *Nano Lett.*, 2009, **9**, 2455.
15 F. Amano, O. Prieto-Mahaney, Y. Terada, T. Yasumoto, T. Shibayama and B. Ohtani, *Chem. Mater.*, 2009, **21**, 2601.
16 D. Zhang, G. Li, X. Yang and J. C. Yu, *Chem. Commun.*, 2009, 4381.
17 G. Liu, H. G. Yang, X. W. Wang, L. Cheng, J. Pan, G. Q. Lu and H. M. Cheng, *J. Am. Chem. Soc.*, 2009, **131**, 12868.
18 M. Liu, L. Pao, L. Zhao, S. Ju, Z. Yan, T. He, C. Zhou and W. Wang, *Chem. Commun.*, 2010, **46**, 1664.
19 F. Lu, W. Cai and Y. Zhang, *Adv. Funct. Mater.*, 2008, **18**, 1047.
20 B. Li, G. Rong, Y. Xie, L. Huang and C. Feng, *Inorg. Chem.*, 2006, **45**, 6404.
21 Y. Ma, S. Weiner and L. Addadi, *Adv. Funct. Mater.*, 2007, **17**, 2693.
22 Z. Liu, X. Zhang, S. Nishimoto, M. Jin, D. A. Tryk, T. Murakami and A. Fujishima, *Langmuir*, 2007, **23**, 10916.
23 E. Hosono, S. Fujihara and T. Kimura, *Electrochim. Acta*, 2004, **49**, 2287.
24 L. Xiao, Y. Yang, J. Yin, Q. Li and L. Zhang, *J. Power Sources*, 2009, **194**, 1089.
25 G. Wu, J. Wang, D. F. Thomas and A. Chen, *Langmuir*, 2008, **24**, 3503.
26 C. Z. Wu, Y. Xie, L. Y. Lei, S. Q. Hu and C. Z. OuYang, *Adv. Mater.*, 2006, **18**, 1727.
27 X. L. Hu, J. C. Yu and J. M. Gong, *J. Phys. Chem. C*, 2007, **111**, 11180.
28 A. Vittadini, A. Selloni, F. P. Rotzinger and M. Gratzel, *Phys. Rev. Lett.*, 1998, **81**, 2954.
29 G. S. Herman, Z. Dohnalek, N. Ruzycki and U. Diebold, *J. Phys. Chem. B*, 2003, **107**, 2788.
30 A. Tilocca and A. Selloni, *J. Phys. Chem. B*, 2004, **108**, 19314.
31 C. Arrouvel, M. Digne, M. Breysse, H. Toulhoat and P. Raybaud, *J. Catal.*, 2004, **222**, 152.
32 A. Selloni, *Nat. Mater.*, 2008, **7**, 613.